

Received March 3, 2020, accepted March 9, 2020, date of publication March 23, 2020, date of current version March 31, 2020.

Digital Object Identifier 10.1109/ACCESS.2020.2982464

# Hybrid-Driven-Based $H_\infty$ Control for Offshore Steel Jacket Platforms in Network Environments

EN-ZHI CAO<sup>1</sup>, ZHIHUI CAI<sup>2</sup>, BAO-LIN ZHANG<sup>1,2</sup> , (Member, IEEE), AND BINRUI WANG<sup>1</sup>

<sup>1</sup>College of Mechanical and Electrical Engineering, China Jiliang University, Hangzhou 310018, China

<sup>2</sup>College of Science, China Jiliang University, Hangzhou 310018, China

Corresponding author: Zhihui Cai (zhcai@cjlu.edu.cn)

This work was supported in part by the Natural Science Foundation of China under Grant 61773356, and in part by the Key Project of Natural Science Foundation of Zhejiang Province of China under Grant LZ19F030001.

**ABSTRACT** This paper investigates the hybrid-driven-based networked control for an offshore steel jacket platform subject to external wave forces. A hybrid driven strategy is introduced to deal with the problem of networked control for offshore platforms. Then, the networked closed-loop system is modeled as a stochastic delay system. Based on this model, a stability criterion is derived using the stochastic control theory and the Lyapunov-Krasovskii functional method. Simulation results show that the hybrid-driven-based networked  $H_\infty$  controller is effective to suppress the vibration of the platform and save the limited network resources as well. Moreover, the designed controller is flexible in terms of maintaining a balance between performance requirements of the offshore platform and the utilization of communication network bandwidth.


**INDEX TERMS** Offshore platform, networked control system,  $H_\infty$  control, stochastic system, hybrid driven strategy.

## I. INTRODUCTION

As one of representative offshore platforms, the offshore steel jacket platform is primarily used in oil and gas extraction. In the presence of sophisticated external disturbances such as wave, earthquake, and wind [1]–[3], offshore operations are often influenced by the excited excessive vibration amplitudes of the platform. Note that the corresponding service life can be extended beyond two times, when the vibration of the platform can be taken a 15 percent reduction [4]. In the last decade, the active control [5]–[10], passive control [11] and semi-active control [12] schemes are applied to the offshore platforms. Due to the flexibility and adaptability, the active control is much easier to satisfy the system performance requirements. Therefore, ever-increasing attention has been paid to active control. To mention a few, to reduce vibration of the platform, a robust mixed  $H_2/H_\infty$  control strategy is proposed [13]. In [8] and [14], the offshore platform is modelled as an uncertain system and some integral sliding mode control schemes are developed. However, the aforementioned approaches are based on traditional point-to-point control architectures and the control components are connected by complex system cabling. Due to the fact that offshore platforms are generally far from land, from the point of view

of increasing system agility and saving control cost, it is necessary to find suitable network-based control methods for offshore platforms.

It should be mentioned that network control systems (NCSs) have some practical advantages such as plug and play equipment and low maintenance cost, and have received a great deal of attention, see [15]–[21]. Compared with the traditional point-to-point control, the network-based control strategy is more effective and feasible for an offshore platform. For example, in [22], a communication network is employed to link the control components of an offshore platform within a closed control loop. Then, a network-based model is established for the platform. In [23], taking actuator faults and external wave forces into consideration, an event-triggering scheme is utilized to save network resources via the networked model of the platform. From transmitting sampled signal point of view, it should be noted that there are main two types of schemes: time-triggering schemes (TTSs) and event-triggering schemes (ETSs). In fact, for NCSs, there are fruitful results on theory and application of TTSs and ETSs, see [24]–[31]. For instance, in [25], the distributed  $H_\infty$  filtering problem is investigated for sensor networks under the TTS and some important results are presented to verify the usefulness of this approach. Based on the ETS, a suitable filter is designed for a class of delay neural networks [28]. Under the TTS, the distributed cooperative control is surveyed for

The associate editor coordinating the review of this manuscript and approving it for publication was Shouguang Wang .

multi-agent systems [30]. In most cases, on the one hand, it is worth pointing out that TTSs are more concerned with the system performance demands such that some inessential data packets are transmitted through the communication network, which wastes the limited network bandwidth. On the other hand, when the bandwidth is inadequate, ETSS can reduce utilization of communication resources by sacrificing the system performance. Obviously, such two schemes are not flexible enough to adapt to different system conditions, where normal networks are suddenly suffered from a congested communication traffic while the favorable performance is always required. To deal with the problem, in [32], a hybrid driven scheme is developed by inheriting advantages of the TTS and ETS. This method provides a good compromise between performance demands and the quality of communication. There are some recent studies [33]–[35] about this hybrid scheme. However, to the best of our knowledge, for the jacket platform systems, how to keep a balance between meeting system performance requirements and saving the restricted network bandwidth is a significant issue, which requires further investigation and motivates this study.

Inspired by [32], a hybrid driven scheme is introduced to investigate the network-based state feedback control problem for the jacket platform subject to external wave forces. The main contributions are summarized as follows:

(i) Different from [22] and [23], under the hybrid-triggering scheme, the network-based model of the jacket platform is deemed as a stochastic system with different delays.

(ii) For the networked jacket platform system, a hybrid-driven-based  $H_\infty$  controller is designed to attenuate the amplitudes of displacement and acceleration, and reduce the utilization of communication resources.

The remainder of this paper is organized as follows. In Section II, a dynamic model is established under the hybrid driven mechanism. The design of a networked controller is developed in Section III. Section IV shows the simulation results. Section V presents some conclusions.

*Notations:*  $P > 0$  means the matrix  $P$  is positive definite.  $\mathbb{E}$  denotes the expectation operator.  $\text{Prob}\{\beta\}$  defines the probability value of stochastic variable  $\beta$ .  $N$  is the set of nonnegative integer. ‘ $T$ ’ and ‘ $-1$ ’ stand for the matrix transpose and matrix inverse.  $\mathbb{R}^{p \times p}$  and  $\mathbb{R}^p$  are the set of all  $p \times p$  real matrices and  $p$ -dimensional Euclidean space.  $L_2[0, +\infty)$  represents the space of square integrable functions.  $\text{diag}\{\dots\}$  and  $I$  denote the diagonal matrix and identity matrix with suitable dimensions.  $H_e\{Z\}$  stands for  $Z + Z^T$ . The symmetric term is given by  $*$ , e.g.,

$$\begin{bmatrix} W_1 & W_2 \\ * & W_3 \end{bmatrix} = \begin{bmatrix} W_1 & W_2 \\ W_2^T & W_3 \end{bmatrix}$$

## II. PROBLEM FORMULATION

### A. THE BASIC MODEL OF A JACKET PLATFORM

An offshore steel jacket platform with an active mass damper (AMD) device is shown in Fig. 1 [5]. The dynamic equations

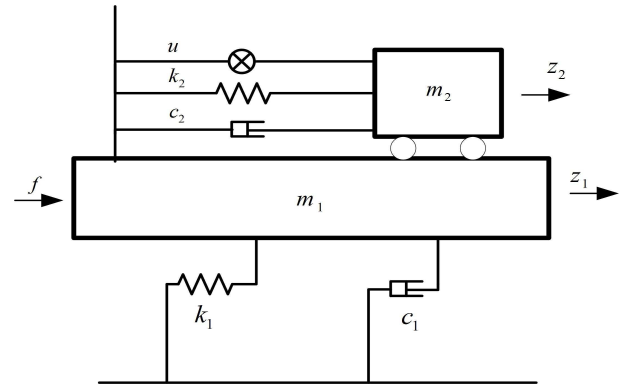


FIGURE 1. A simplified offshore platform [5].

of the simplified jacket platform can be obtained as

$$\begin{cases} m_1 \ddot{z}_1(t) = -c_1 \dot{z}_1(t) - k_1 z_1(t) + k_2 z_2(t) \\ \quad - k_2 z_1(t) + c_2 \dot{z}_2(t) - c_2 \dot{z}_1(t) \\ \quad + f(t) - u(t) \\ m_2 \ddot{z}_2(t) = -c_2 \dot{z}_2(t) + c_2 \dot{z}_1(t) - k_2 z_2(t) \\ \quad + k_2 z_1(t) + u(t) \end{cases} \quad (1)$$

where  $u(t)$  represents control force of the system.  $f(t)$  stands for the external wave force,  $z_1(t)$  and  $z_2(t)$  stand for the displacements of the offshore platform and AMD, respectively;  $m_1$ ,  $k_1$  and  $c_1$  are the mass, stiffness and damping of the platform, respectively;  $m_2$ ,  $k_2$  and  $c_2$  are the mass, stiffness and damping of the AMD device, respectively.

Let

$$\begin{cases} x_1(t) = z_1(t), \quad x_2(t) = z_2(t) \\ x_3(t) = \dot{z}_1(t), \quad x_4(t) = \dot{z}_2(t) \\ x(t) = [x_1(t) \quad x_2(t) \quad x_3(t) \quad x_4(t)]^T \end{cases} \quad (2)$$

Then, from (1) and (2), the state space system equation is shown as

$$\dot{x}(t) = Ax(t) + Bu(t) + D_0 f(t), \quad x(0) = x_0 \quad (3)$$

where

$$\begin{cases} A = \begin{bmatrix} 0 & 0 & 1 & 0 \\ 0 & 0 & 0 & 1 \\ -\frac{k_1 + k_2}{m_1} & \frac{k_2}{m_1} & -\frac{c_1 + c_2}{m_1} & \frac{c_2}{m_1} \\ \frac{k_2}{m_2} & -\frac{k_2}{m_2} & \frac{c_2}{m_2} & -\frac{c_2}{m_2} \end{bmatrix} \\ B = \begin{bmatrix} 0 & 0 & -\frac{1}{m_1} & \frac{1}{m_2} \end{bmatrix}^T \\ D_0 = \begin{bmatrix} 0 & 0 & \frac{1}{m_1} & 0 \end{bmatrix}^T \end{cases} \quad (4)$$

The controlled output is given as

$$z(t) = C_1 x(t) + D_1 f(t) \quad (5)$$

Now, a communication network is used to the remote control of the offshore platform (3). Assume that the sensor is clock-driven, the actuator and controller are event-driven, and the state information is sent with a single packet, while packet disorders, network-induced delays and packet dropouts are not considered.

**B. THE NETWORK-BASED MODEL OF THE JACKET PLATFORM UNDER A HYBRID-TRIGGERING MECHANISM**

The networked state feedback control law  $u(t)$  can be designed as

$$u(t) = Kx(t_k h), \quad t \in [t_k h, t_{k+1} h), \quad k \in N \quad (6)$$

where  $K$  is a controller gain matrix,  $h > 0$  is the sampling period and  $t_k h$  is the sampling instant which reaches the actuator successfully.

From the view of data transmission in networked control systems (NCSs), if the time-triggering mechanism is selected, the all sampled signals are transmitted over the real-time network. In this case, the control law (6) can be rewritten as

$$u_1(t) = Kx(kh), \quad t \in [t_k h, t_{k+1} h), \quad k \in N \quad (7)$$

Define  $\tau_1(t) = t - kh$ . Then, the control signal (7) is equivalent to

$$u_1(t) = Kx(t - \tau_1(t)), \quad t \in [t_k h, t_{k+1} h) \quad (8)$$

where  $\tau_1(t) \in [0, h)$  and  $\dot{\tau}_1(t) = 1$ .

It is clear that this mechanism is usually applied to obtain a desired control performance for NCSs. However, some unimportant control data packets are used in the scheme such that communicate network resources are wasted.

When the event-triggering mechanism is selected, we define the signal transmission error vector as

$$e_k(t) = x(t_k h) - x(t_k h + mh), \quad m \in N^+ \quad (9)$$

Then, a triggering condition is designed as

$$e_k^T(t) W e_k(t) \leq \sigma x^T(t_k h + mh) W x(t_k h + mh) \quad (10)$$

where the scalar  $\sigma \in (0, 1)$  and matrix  $W > 0$ . Clearly, if the above condition is satisfied, the current sampled signal  $x(t_k h + mh)$  will not be transmitted.

Let the time interval

$$[t_k h, t_{k+1} h) = \bigcup_{m=0}^l \Upsilon_m \quad (11)$$

where  $\Upsilon_m = [t_k h + mh, t_k h + mh + h)$ ,  $l = t_{k+1} - t_k - 1$ ,  $m = 0, 1, \dots, l$ .

Similar to [36], denote  $\tau_2(t) = t - t_k h - mh$ . Then the control input (6) can be written as

$$u_2(t) = K[x(t - \tau_2(t)) + e_k(t)], \quad t \in [t_k h, t_{k+1} h) \quad (12)$$

where  $\tau_2(t) \in [0, h)$  and  $\dot{\tau}_2(t) = 1$ .

Under the event-triggering scheme, note that the network and energy resources are saved particularly, while the

corresponding performance of the control system may be sacrificed.

In what follows, to keep balance between system performance and communicate network resources, motivated by [32], a hybrid-triggering scheme is introduced for the offshore platform.

Combining (8) and (12), the control law (6) can be expressed as

$$u(t) = \alpha(t)u_1(t) + (1 - \alpha(t))u_2(t) \quad (13)$$

where  $\alpha(t)$  is a Bernoulli random variable with following probability

$$\begin{cases} \text{Prob} \{ \alpha(t) = 1 \} = \bar{\alpha} \\ \text{Prob} \{ \alpha(t) = 0 \} = 1 - \bar{\alpha} \end{cases} \quad (14)$$

with  $\bar{\alpha} \in [0, 1]$ . Then, from (13), the closed-loop system (3) is modeled as

$$\begin{cases} \dot{x}(t) = Ax(t) + \alpha(t)BKx(t - \tau_1(t)) \\ \quad + (1 - \alpha(t))BK[x(t - \tau_2(t)) + e_k(t)] \\ \quad + D_0 f(t) \\ x(0) = x_0, \quad t \in [t_k h, t_{k+1} h), \quad k \in N \end{cases} \quad (15)$$

which is a stochastic system with two delays  $\tau_1(t)$  and  $\tau_2(t)$ .

*Remark 1:* The Bernoulli random variable  $\alpha(t)$  can be viewed as a switched parameter with a certain probability. Thus, this hybrid driven scheme can switch randomly between the event-triggering scheme and time-triggering scheme, which is the special nature of this scheme.

The aim of this paper is to design a hybrid-driven-based networked  $H_\infty$  controller such that the offshore platform system (15) is internally mean square asymptotically stable (MSAS) and satisfies

$$\mathbb{E} \left\{ z^T(t) z(t) \right\} < \gamma^2 \mathbb{E} \left\{ f^T(t) f(t) \right\} \quad (16)$$

for a prescribed  $\gamma > 0$  and the external wave  $f(t) \in L_2[0, +\infty)$ .

To obtain the main results, the following Lemma is necessary.

*Lemma 1:* [37] For a symmetric matrix  $X \in \mathbb{R}^{n \times n}$  and a matrix  $U \in \mathbb{R}^{n \times n}$  such that

$$\begin{bmatrix} X & U \\ * & X \end{bmatrix} \geq 0$$

the following inequality holds for  $d(t) \in [d_1, d_2]$  and a vector function  $\dot{\omega} : [t - d_2, t - d_1] \rightarrow \mathbb{R}^n$

$$(d_2 - d_1) \int_{t-d_2}^{t-d_1} \dot{\omega}^T(s) X \dot{\omega}(s) ds \geq \xi^T(t) \begin{bmatrix} X & U \\ * & X \end{bmatrix} \xi(t)$$

where  $\xi(t) = \begin{bmatrix} \omega(t - d_1) - \omega(t - d(t)) \\ \omega(t - d(t)) - \omega(t - d_2) \end{bmatrix}$ .

III. CONTROLLER DESIGN

In this section, a hybrid-driven-based networked  $H_\infty$  controller is designed. The following proposition is given to illustrate the existence of this controller.

*Proposition 1:* For prescribed scalars  $\gamma > 0, h > 0, \sigma \in (0, 1), \bar{\alpha} \in [0, 1]$ , the network-based system (15) is MSAS with  $f(t) = 0$  and the  $H_\infty$  performance (16) is ensured, if there exist  $4 \times 4$  matrices  $P > 0, W > 0, Q_i > 0, R_i > 0, S_i, (i = 1, 2)$  and a  $1 \times 4$  matrix  $K$  such that

$$\begin{bmatrix} \Psi & \eta_1 & \eta_2 & \eta_3 & \eta_4 \\ * & -\gamma^2 I & hD_0^T P & 0 & D_1^T \\ * & * & -P\mathcal{R}^{-1}P & 0 & 0 \\ * & * & * & -P\mathcal{R}^{-1}P & 0 \\ * & * & * & * & -I \end{bmatrix} < 0 \quad (17)$$

$$\begin{bmatrix} R_i & S_i \\ * & R_i \end{bmatrix} \geq 0, \quad (i = 1, 2) \quad (18)$$

where

$$\Psi = \begin{bmatrix} \Pi_{11} & \Pi_{12} & \Pi_{13} & S_1 + S_2 & \Pi_{15} \\ * & \Pi_{22} & 0 & R_1 - S_1 & 0 \\ * & * & \Pi_{33} & R_2 - S_2 & 0 \\ * & * & * & \Pi_{44} & 0 \\ * & * & * & * & -W \end{bmatrix} \quad (19)$$

$$\eta_1^T = [D_0^T P \ 0 \ 0 \ 0 \ 0], \quad \eta_4^T = [C_1 \ 0 \ 0 \ 0 \ 0]$$

$$\eta_2^T = [hPA \ h\bar{\alpha}\Theta \ h(1-\bar{\alpha})\Theta \ 0 \ h(1-\bar{\alpha})\Theta]$$

$$\eta_3^T = [0 \ h\delta\Theta \ -h\delta\Theta \ 0 \ -h\delta\Theta]$$

with

$$\begin{cases} \Pi_{11} = H_e\{PA\} + Q - \mathcal{R}, \quad \Pi_{12} = \bar{\alpha}\Theta + R_1 - S_1 \\ \Pi_{13} = (1 - \bar{\alpha})\Theta + R_2 - S_2, \quad \Pi_{15} = (1 - \bar{\alpha})\Theta \\ \Pi_{22} = H_e\{S_1 - R_1\}, \quad \Theta = PBK, \quad \delta = \sqrt{\bar{\alpha}(1-\bar{\alpha})} \\ \Pi_{33} = \sigma W + H_e\{S_2 - R_2\}, \quad \mathcal{R} = R_1 + R_2 \\ \Pi_{44} = -(Q + \mathcal{R}), \quad Q = Q_1 + Q_2 \end{cases}$$

*Proof:* Construct a Lyapunov-Krasovskii function candidate as

$$\begin{aligned} V(t) &= x^T(t)Px(t) \\ &+ \int_{t-h}^t x^T(s)Qx(s)ds \\ &+ h \int_{-h}^0 \int_{t+\theta}^t \dot{x}^T(s)\mathcal{R}\dot{x}(s)dsd\theta \end{aligned} \quad (20)$$

where  $P > 0, Q = Q_1 + Q_2 > 0, \mathcal{R} = R_1 + R_2 > 0$ .

Taking the derivative of  $V(t)$  and taking mathematical expectation, we obtain

$$\begin{aligned} \mathbb{E}\{\dot{V}(t)\} &= \mathbb{E}\left\{2x^T(t)P\dot{x}(t)\right\} + h^2\mathbb{E}\left\{\dot{x}^T(t)\mathcal{R}\dot{x}(t)\right\} \\ &+ x^T(t)Qx(t) - x^T(t-h)Qx(t-h) \\ &- h \int_{t-h}^t \dot{x}^T(s)\mathcal{R}\dot{x}(s)ds \end{aligned} \quad (21)$$

Notice that

$$\begin{aligned} h \int_{t-h}^t \dot{x}^T(s)R_i\dot{x}(s)ds &= h \int_{t-\tau_i(t)}^t \dot{x}^T(s)R_i\dot{x}(s)ds \\ &+ h \int_{t-h}^{t-\tau_i(t)} \dot{x}^T(s)R_i\dot{x}(s)ds \end{aligned} \quad (22)$$

By Lemma 1 and Jensen's inequality, if (18) holds, we have

$$h \int_{t-h}^t \dot{x}^T(s)R_i\dot{x}(s)ds \geq \Lambda_i^T \begin{bmatrix} R_i & S_i \\ * & R_i \end{bmatrix} \Lambda_i \quad (23)$$

where

$$\Lambda_i = \begin{bmatrix} x(t) - x(t - \tau_i(t)) \\ x(t - \tau_i(t)) - x(t - h) \end{bmatrix}, \quad i = 1, 2 \quad (24)$$

It is clear that the dynamic equation (15) can be rewritten as

$$\begin{aligned} \dot{x}(t) &= Ax(t) + D_0f(t) + \bar{\alpha}BKx(t - \tau_1(t)) \\ &+ (1 - \bar{\alpha})B[Kx(t - \tau_2(t)) + Ke_k(t)] \\ &+ (\alpha(t) - \bar{\alpha})B[Kx(t - \tau_1(t)) - Kx(t - \tau_2(t)) \\ &- Ke_k(t)] \end{aligned} \quad (25)$$

Note that

$$\begin{cases} \mathbb{E}\{\alpha(t)\} = \bar{\alpha}, \quad \mathbb{E}\{\alpha(t) - \bar{\alpha}\} = 0 \\ \mathbb{E}\{(\alpha(t) - \bar{\alpha})^2\} = \bar{\alpha}(1 - \bar{\alpha}) \end{cases} \quad (26)$$

Then, from (25) and (26), we obtain

$$\mathbb{E}\left\{\dot{x}^T(t)\mathcal{R}\dot{x}(t)\right\} = F_1^T\mathcal{R}F_1 + \delta^2F_2^T\mathcal{R}F_2 \quad (27)$$

where

$$\begin{cases} \delta^2 = \bar{\alpha}(1 - \bar{\alpha}) \\ F_1 = Ax(t) + \bar{\alpha}BKx(t - \tau_1(t)) \\ \quad + (1 - \bar{\alpha})BK[x(t - \tau_2(t)) + e_k(t)] \\ \quad + D_0f(t) \\ F_2 = BKx(t - \tau_1(t)) - BKx(t - \tau_2(t)) \\ \quad - BKe_k(t) \end{cases} \quad (28)$$

Let  $f(t) = 0$ . Then adding the term  $e_k^T(t)We_k(t) - e_k^T(t)We_k(t)$  to the right-hand side of (21), and combining (21)-(28) and (15), one yields

$$\mathbb{E}\{\dot{V}(t)\} \leq \xi_1^T(t)[\Psi + \Xi_1]\xi_1(t) \quad (29)$$

where

$$\begin{aligned} \xi_1^T(t) &= [x^T(t) \ x^T(t - \tau_1(t)) \ x^T(t - \tau_2(t)) \ x^T(t - h) \ e_k^T(t)] \\ \Xi_1 &= \eta_2(P^{-1}\mathcal{R}P^{-1})\eta_2^T + \eta_3(P^{-1}\mathcal{R}P^{-1})\eta_3^T \text{ with } \eta_i^T (i = 2, 3) \\ &\text{and } \Psi \text{ is defined in (19).} \end{aligned}$$

Note that if  $\Psi + \Xi_1 < 0$  holds, then we have  $\mathbb{E}\{\dot{V}(t)\} < 0$ . By Schur complements,  $\Psi + \Xi_1 < 0$  is equivalent to

$$\begin{bmatrix} \Psi & \eta_2 & \eta_3 \\ * & -P\mathcal{R}^{-1}P & 0 \\ * & * & -P\mathcal{R}^{-1}P \end{bmatrix} < 0 \quad (30)$$

In fact, the inequality (30) can be ensured by the inequality (17). Then, the system (15) with  $f(t) = 0$  is MSAS.

Set  $f(t) \neq 0$  in the system (15) and

$$\xi_2^T(t) = [\xi_1^T(t) \quad f^T(t)] \quad (31)$$

Then, from (5) and (21), one has

$$\begin{aligned} \mathbb{E}\{\dot{V}(t)\} + \mathbb{E}\{z^T(t)z(t)\} - \gamma^2 \mathbb{E}\{f^T(t)f(t)\} \\ \leq \xi_2^T(t)[\Phi + \Xi_2]\xi_2(t) \end{aligned} \quad (32)$$

where

$$\begin{aligned} \Phi &= \begin{bmatrix} \Psi & \eta_1 \\ * & -\gamma^2 I \end{bmatrix} \\ \Xi_2 &= \begin{bmatrix} \eta_2 \\ hD_0^T P \end{bmatrix} [P^{-1} \mathcal{R} P^{-1}] \begin{bmatrix} \eta_2 \\ hD_0^T P \end{bmatrix}^T \\ &+ \begin{bmatrix} \eta_3 \\ 0 \end{bmatrix} [P^{-1} \mathcal{R} P^{-1}] \begin{bmatrix} \eta_3 \\ 0 \end{bmatrix}^T \\ &+ \begin{bmatrix} \eta_4 \\ D_1^T \end{bmatrix} \begin{bmatrix} \eta_4 \\ D_1^T \end{bmatrix}^T \end{aligned}$$

with  $\Psi$  and  $\eta_i$  ( $i = 1, 2, 3, 4$ ) are given by (19). Then, by Schur complements, if matrix inequalities (17) and (18) hold, we have

$$\Phi + \Xi_2 < 0 \quad (33)$$

Further, from (33), yields

$$\mathbb{E}\{\dot{V}(t)\} + \mathbb{E}\{z^T(t)z(t)\} - \gamma^2 \mathbb{E}\{f^T(t)f(t)\} < 0 \quad (34)$$

It is obvious from (34) that

$$\mathbb{E}\left\{ \int_0^{+\infty} z^T(t)z(t)dt \right\} < \mathbb{E}\left\{ \int_0^{+\infty} \gamma^2 f^T(t)f(t)dt \right\} \quad (35)$$

Then, the  $H_\infty$  performance index (16) of the system (15) is guaranteed. The proof is complete.

Note that the matrix inequality (17) is nonlinear. So let

$$\begin{cases} X = P^{-1}, \quad Y = KP^{-1}, \quad \bar{R}_i = P^{-1}R_iP^{-1} \\ \bar{Q}_i = P^{-1}Q_iP^{-1}, \quad \bar{S}_i = P^{-1}S_iP^{-1} \quad (i = 1, 2) \\ \bar{W} = P^{-1}WP^{-1} \end{cases} \quad (36)$$

Using the inequality  $-P\mathcal{R}^{-1}P \leq -2v_1P + v_1^2\mathcal{R}$ , and pre- and post-multiply (17) by  $\text{diag}\{X, X, X, X, X, I, X, X, I\}$ , (18) by  $\text{diag}\{X, X\}$ , and its transpose, respectively. Then, the inequality (17) is linearized and the following Proposition is given.

**Proposition 2:** For given scalars  $v_1 > 0, h > 0, \gamma > 0, \sigma \in (0, 1), \bar{\alpha} \in [0, 1]$ , if there exist  $4 \times 4$  matrices  $X > 0, \bar{W} > 0, \bar{Q}_i > 0, \bar{R}_i > 0, \bar{S}_i, (i = 1, 2)$  and a  $1 \times 4$  matrix  $Y$  such that

$$\begin{bmatrix} \bar{\Psi} & \bar{\eta}_1 & \bar{\eta}_2 & \bar{\eta}_3 & \bar{\eta}_4 \\ * & -\gamma^2 I & hD_0^T & 0 & D_1^T \\ * & * & \Omega & 0 & 0 \\ * & * & * & \Omega & 0 \\ * & * & * & * & -I \end{bmatrix} < 0 \quad (37)$$

$$\begin{bmatrix} \bar{R}_i & \bar{S}_i \\ * & \bar{R}_i \end{bmatrix} \geq 0, \quad (i = 1, 2) \quad (38)$$

where

$$\begin{cases} \bar{\Psi} = \begin{bmatrix} \bar{\Pi}_{11} & \bar{\Pi}_{12} & \bar{\Pi}_{13} & \bar{S}_1 + \bar{S}_2 & \bar{\Pi}_{15} \\ * & \bar{\Pi}_{22} & 0 & \bar{R}_1 - \bar{S}_1 & 0 \\ * & * & \bar{\Pi}_{33} & \bar{R}_2 - \bar{S}_2 & 0 \\ * & * & * & \bar{\Pi}_{44} & 0 \\ * & * & * & * & -\bar{W} \end{bmatrix} \\ \bar{\eta}_1^T = [D_0^T \quad 0 \quad 0 \quad 0 \quad 0] \\ \bar{\eta}_2^T = [hAX \quad h\bar{\alpha}BY \quad h(1 - \bar{\alpha})BY \quad 0 \quad h(1 - \bar{\alpha})BY] \\ \bar{\eta}_3^T = [0 \quad h\delta BY \quad -h\delta BY \quad 0 \quad -h\delta BY] \\ \bar{\eta}_4^T = [C_1X \quad 0 \quad 0 \quad 0 \quad 0] \\ \Omega = -2v_1X + v_1^2\bar{\mathcal{R}} \end{cases}$$

with

$$\begin{cases} \bar{Q} = \bar{Q}_1 + \bar{Q}_2, \quad \bar{\mathcal{R}} = \bar{R}_1 + \bar{R}_2 \\ \bar{\Pi}_{11} = H_e\{AX\} + \bar{Q} - \bar{\mathcal{R}}, \quad \delta = \sqrt{\bar{\alpha}(1 - \bar{\alpha})} \\ \bar{\Pi}_{12} = \bar{\alpha}BY + \bar{R}_1 - \bar{S}_1, \quad \Pi_{33} = \sigma\bar{W} + H_e\{\bar{S}_2 - \bar{R}_2\} \\ \bar{\Pi}_{13} = (1 - \bar{\alpha})BY + \bar{R}_2 - \bar{S}_2, \quad \Pi_{22} = H_e\{\bar{S}_1 - \bar{R}_1\} \\ \bar{\Pi}_{15} = (1 - \bar{\alpha})BY, \quad \Pi_{44} = -(\bar{Q} + \bar{\mathcal{R}}) \end{cases}$$

Then, the system (15) is internally MSAS and the  $H_\infty$  index (16) can be guaranteed. The controller gain  $K = YX^{-1}$  and trigger parameter matrix  $W = X^{-1}\bar{W}X^{-1}$ .

**Remark 2:** Similar to [32], specially, in Proposition 2, if the scalar  $\bar{\alpha} = 0$ , the hybrid driven scheme is changed to the event-triggering mechanism. If the scalars  $\bar{\alpha} = 1$  and  $\sigma = 0$ , the time-triggering mechanism is created. In fact, in some cases where the network bandwidth is adequate and the system performance is more concerned, choosing a bigger scalar  $\bar{\alpha}$  can reach the control objective. Moreover, when communication resources are scarce and control performance demands are not too high, it is a good option to take a smaller scalar  $\bar{\alpha}$ . Obviously, the hybrid driven scheme can combine advantages of the time-triggering scheme and event-triggering scheme. Thus, a good compromise can be obtained in terms of choosing communication schemes. This method is more flexible in dealing with different types of systems.

**Remark 3:** Different from the event-triggering scheme for the offshore platform [23], in this paper, the development of this hybrid mechanism depends closely on the random variable  $\alpha(t)$ . In this situation, this method can reduce the utilization of communication resources to a similar level as the event-triggering scheme [23].

**Remark 4:** In contrast with [32], external disturbances are taken into account and some new stability conditions are presented in Proposition 2. It is found from simulation results (Section IV) that the Zeno behavior does not happen on the offshore platform. The proposed method may be applied to repetitive control systems [38], [39] to deal with external disturbances.

#### IV. SIMULATION RESULTS

In this section, to show the effectiveness of the proposed control scheme, a hybrid-driven-based networked  $H_\infty$  controller



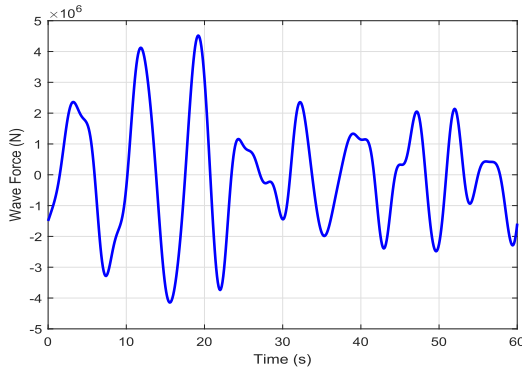


FIGURE 2. The external irregular wave force [23].

(HDNHC) is designed first. Then, the HDNHC is applied to an offshore platform, and the performance of the offshore platform with the HDNHC will be investigated. In addition, the designed HDNHC will be compared with the traditional  $H_\infty$  controller (HIC) [7], an event-based networked  $H_\infty$  controller (ENHC), and a time-based networked  $H_\infty$  controller (TNHC), respectively.

The parameters of the platform are taken from [5]. Then, the system matrices in (4) can be obtained as

$$A = \begin{bmatrix} 0 & 0 & 1.0000 & 0 \\ 0 & 0 & 0 & 1.000 \\ -4.2289 & 0.0403 & -0.0899 & 0.008 \\ 4.0297 & -4.0297 & 0.8030 & -0.8030 \end{bmatrix}$$

$$B = 10^{-4} \times \begin{bmatrix} 0 & 0 & -0.0013 & 0.1278 \end{bmatrix}^T$$

$$D_0 = 10^{-6} \times \begin{bmatrix} 0 & 0 & 0.1278 & 0 \end{bmatrix}^T$$

The matrices  $C_1$  and  $D_1$  in (5) are given as

$$C_1 = \begin{bmatrix} 1 & 0 & 0 & 0 \\ 0 & 0 & 1 & 0 \end{bmatrix}, \quad D_1 = \begin{bmatrix} 0.1 \\ 0 \end{bmatrix}$$

The external wave force data is computed as [23], and the response curve of the wave force is presented in Fig. 2.

### A. PERFORMANCE OF THE OFFSHORE PLATFORM WITH AN HDNHC

To design an HDNHC, let  $h = 0.1$ ,  $\gamma = 0.12$ ,  $\sigma = 0.7$ ,  $\bar{\alpha} = 0.15$ , and  $v_1 = 0.1$ . By Proposition 2, we obtain the matrix  $W$  in the event-triggering condition (10) and the gain matrix  $K$  of the controller as

$$W = \begin{bmatrix} 878.4914 & -0.4821 & 40.3216 & -20.3208 \\ -0.4821 & 0.3779 & 2.4382 & 0.0427 \\ 40.3216 & 2.4382 & 19.6309 & -0.7207 \\ -20.3208 & 0.0427 & -0.7207 & 0.4840 \end{bmatrix}$$

$$K = 10^6 \times \begin{bmatrix} 4.5941 & 0.0064 & 0.2729 & -0.1029 \end{bmatrix}$$

Under the HDNHC, it can be computed that the peak values of displacement and acceleration responses of the offshore platform are reduced from 0.2829 m and 0.7987 m/s<sup>2</sup>

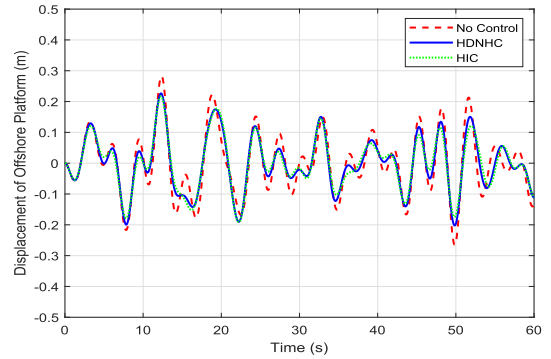


FIGURE 3. Displacement of the offshore platform under different controllers.

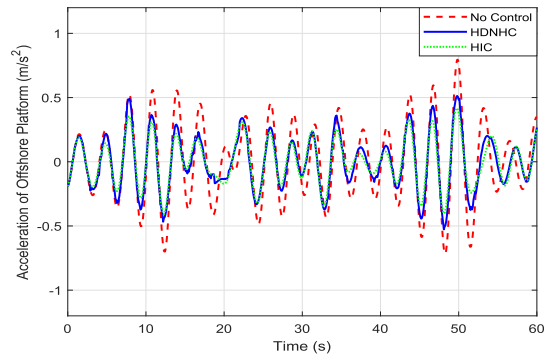


FIGURE 4. Acceleration of the offshore platform under different controllers.

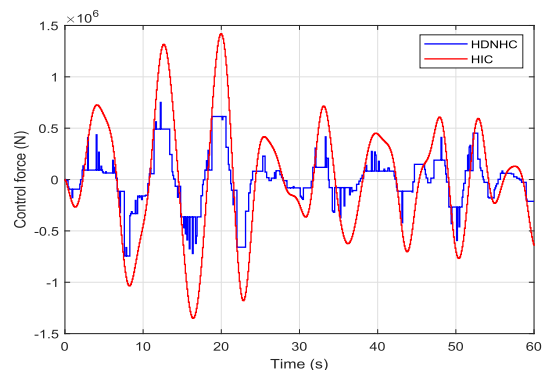


FIGURE 5. Control force under different controllers.

to 0.2258 m and 0.5360 m/s<sup>2</sup>, respectively; the root mean square (RMS) values of displacement and acceleration responses of the system are reduced from 0.1025 m and 0.3088 m/s<sup>2</sup> to 0.0869 m and 0.2041 m/s<sup>2</sup>, respectively; The peak and RMS values of control force by the HDNHC are  $7.8314 \times 10^5$  N and  $2.3549 \times 10^5$  N, respectively. It shows that the proposed control scheme is effective to attenuate the vibration amplitudes of the offshore platform. Consequently, the stability of the offshore platform and the safety of the staff on the platform are improved.

Depicted in Figs. 3 and 4 are response curves of displacement and acceleration of the platform with HDNHC, HIC [7] and without controller. Fig. 5 is the curves of control force

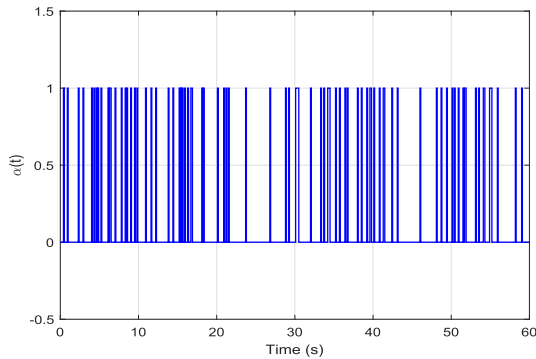


FIGURE 6. Bernoulli stochastic variable  $\alpha(t)$  with  $\bar{\alpha} = 0.15$ .

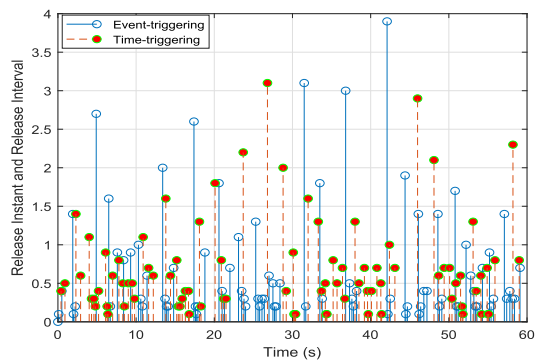


FIGURE 7. Release instants and intervals of data packets versus time.

by HDNHC and HIC [7]. From Figs. 3-5, one can observe that under HDNHC and HIC, the vibration amplitudes of the offshore platform are almost the same, while the control force required by HDNHC is smaller than the one by HIC [7]. It means that, from the point of view of saving control cost, the designed HDNHC is better than the HIC [7].

Fig. 6 provides the curve of Bernoulli stochastic function  $\alpha(t)$  with  $\bar{\alpha} = 0.15$ . Based on the given Bernoulli function, the event-trigger and time-trigger are switched stochastically during the control of HDNHC. In this situation, it can be computed that in the all 601 data packets, only 168 packets are transmitted, and the transmission rate (TR) of the data packets is only about 28% in the case of HDNHC. The release instants and intervals of data packets versus time are given by Fig. 7. This implies that under the HDNHC, the communication network resources are then saved significantly.

### B. COMPARISONS OF THE HDNHC, ENHC, AND TNHC

For comparison purpose, now we turn to design an ENHC and a TNHC. For this, let  $\bar{\alpha} = 0$ , and set the same values of other parameters as the ones in subsection IV-A. Then, By Proposition 2, we obtain the matrices  $W$  and  $K$  as

$$W = \begin{bmatrix} 2007.6 & 3.0913 & 128.1035 & -39.2604 \\ 3.0913 & 0.2578 & 1.9467 & -0.0384 \\ 128.1035 & 1.9467 & 22.6547 & -2.3429 \\ -39.2604 & -0.0384 & -2.3429 & 0.7810 \end{bmatrix}$$

$$K = 10^6 \times \begin{bmatrix} 6.3849 & 0.0131 & 0.4335 & -0.1232 \end{bmatrix}$$

TABLE 1. Peak values of displacement, acceleration response of the offshore platform and the control force in different cases.

Controllers	$P_d$ (m)	$P_a$ (m/s <sup>2</sup> )	$P_u$ (10 <sup>5</sup> N)
No Control	0.2829	0.7987	/
ENHC	0.2264	0.4582	12.214
HDNHC	0.2258	0.5360	7.8314
TNHC	0.2241	0.4807	5.3506

TABLE 2. RMS values of displacement, acceleration response of the offshore platform and the control force in different cases.

Controller	$R_d$ (m)	$R_a$ (m/s <sup>2</sup> )	$R_u$ (10 <sup>5</sup> N)
No Control	0.1025	0.3088	/
ENHC	0.0871	0.2048	2.9000
HDNHC	0.0869	0.2041	2.3549
TNHC	0.0864	0.1959	2.1998

Set  $\sigma = 0$ ,  $\gamma = 5$ ,  $h = 0.1$ , and  $\bar{\alpha} = 1$ . Then by Proposition 2 again, one yields a TNHC with the gain matrix  $K$  as

$$K = 10^6 \times \begin{bmatrix} 3.2708 & -0.0039 & 0.1986 & -0.0737 \end{bmatrix}$$

When the designed ENHC and TNHC are applied to the offshore platform respectively, the corresponding peak and RMS values of the vibration amplitudes of the platform and the control force are computed and listed in Tables 1 and 2, where  $P_d$  and  $P_a$  are peak values of displacement and acceleration responses of the system respectively,  $P_u$  represents peak value of the control force;  $R_d$  and  $R_a$  are RMS values of displacement and acceleration responses of the platform respectively,  $R_u$  represents the RMS value of the control force.

From Tables 1 and 2, one can observe that under the HDNHC, ENHC, and TNHC, the controlled peak and RMS values of oscillation amplitudes of the offshore platform are almost in the same level, while the control force required are different. In fact, the control cost required by HDNHC is greater than the one by TNHC while less than that by ENHC. Notice that the TR for HDNHC is 28%, which is larger than the one for ENHC (15%). Obviously, ENHC can effectively save network resources, however, it requires more control cost. TNHC needs less control cost while it may consume more network resources. In this situation, HDNHC provides a flexible option to balance control force and the network resources.

### V. CONCLUSION

In this paper, the networked control scheme with hybrid driven mechanisms has been presented for the offshore platform. Some sufficient conditions have been proposed to guarantee the existence of the hybrid-driven-based networked  $H_\infty$  controller. Simulation results have been given to demonstrate the effectiveness of the proposed control schemes. Notice that the network security is very important and unavoidable for the offshore platform. Therefore, the potential issues for the vibration control of offshore platforms may mainly focus on the networked system modeling

and control methods design by considering the influence of cyber attacks on the system.

## REFERENCES

- [1] H. Ma, G.-Y. Tang, and Y.-D. Zhao, "Feedforward and feedback optimal control for offshore structures subjected to irregular wave forces," *Ocean Eng.*, vol. 33, nos. 8–9, pp. 1105–1117, Jun. 2006.
- [2] H. Ma, G.-Y. Tang, and X.-Q. Ding, "Modified-transformation-based networked controller for offshore platforms under multiple overloads," *Ocean Eng.*, vol. 190, Oct. 2019, Art. no. 106392, doi: [10.1016/j.oceaneng.2019.106392](https://doi.org/10.1016/j.oceaneng.2019.106392).
- [3] B.-L. Zhang, Q.-L. Han, and X.-M. Zhang, "Recent advances in vibration control of offshore platforms," *Nonlinear Dyn.*, vol. 89, no. 2, pp. 755–771, Jul. 2017.
- [4] J. Ou, X. Long, Q. S. Li, and Y. Q. Xiao, "Vibration control of steel jacket offshore platform structures with damping isolation systems," *Eng. Struct.*, vol. 29, no. 7, pp. 1525–1538, Jul. 2007.
- [5] H. J. Li, S.-L. James Hu, and C. Jakubiak, "H<sub>2</sub> active vibration control for offshore platform subjected to wave loading," *J. Sound Vib.*, vol. 263, no. 4, pp. 709–724, Jun. 2003.
- [6] X.-M. Zhang, Q.-L. Han, and D. Han, "Effects of small time-delays on dynamic output feedback control of offshore steel jacket structures," *J. Sound Vib.*, vol. 330, no. 16, pp. 3883–3900, Aug. 2011.
- [7] B.-L. Zhang and G.-Y. Tang, "Active vibration H<sub>∞</sub> control of offshore steel jacket platforms using delayed feedback," *J. Sound Vib.*, vol. 332, no. 22, pp. 5662–5677, Oct. 2013.
- [8] B.-L. Zhang, L. Ma, and Q.-L. Han, "Sliding mode control for offshore steel jacket platforms subject to nonlinear self-excited wave force and external disturbance," *Nonlinear Anal.-Real*, vol. 14, no. 1, pp. 163–178, Feb. 2013.
- [9] B.-L. Zhang, Z. Cai, S. Gao, and G.-Y. Tang, "Delayed proportional-integral control for offshore steel jacket platforms," *J. Franklin Inst.*, vol. 356, no. 12, pp. 6373–6387, Aug. 2019.
- [10] S. Huang, M. Cai, and Z. Xiang, "Robust sampled-data H<sub>∞</sub> control for offshore platforms subject to irregular wave forces and actuator saturation," *Nonlin. Dyn.*, vol. 88, no. 4, pp. 2705–2721, Feb. 2017.
- [11] A. A. Golareshani and A. Gholizad, "Passive devices for wave induced vibration control in offshore steel jacket platforms," *Scientia Iranica*, vol. 16, no. 6, pp. 443–456, Nov. 2009.
- [12] T. Pinkaew and Y. Fujino, "Effectiveness of semi-active tuned mass dampers under harmonic excitation," *Eng. Struct.*, vol. 23, no. 7, pp. 850–856, Jul. 2001.
- [13] J. S. Yang, "Robust mixed H<sub>2</sub>/H<sub>∞</sub> active control for offshore steel jacket platform," *Nonlinear Dyn.*, vol. 78, no. 2, pp. 1503–1514, Oct. 2014.
- [14] B.-L. Zhang, Q.-L. Han, X.-M. Zhang, and X. Yu, "Sliding mode control with mixed current and delayed states for offshore steel jacket platforms," *IEEE Trans. Control Syst. Technol.*, vol. 22, no. 5, pp. 1769–1783, Sep. 2014.
- [15] X.-M. Zhang, Q.-L. Han, X. Ge, D. Ding, L. Ding, D. Yue, and C. Peng, "Networked control systems: A survey of trends and techniques," *IEEE/CAA J. Automatica Sinica*, vol. 7, no. 1, pp. 1–17, Jan. 2020.
- [16] H.-H. Lian, S.-P. Xiao, Z. Wang, X.-H. Zhang, and H.-Q. Xiao, "Further results on sampled-data synchronization control for chaotic neural networks with actuator saturation," *Neurocomputing*, vol. 346, pp. 30–37, Jun. 2019.
- [17] J. Liu, W. Suo, L. Zha, E. Tian, and X. Xie, "Security distributed state estimation for nonlinear networked systems against DoS attacks," *Int. J. Robust Nonlinear Control*, vol. 30, no. 3, pp. 1156–1180, Feb. 2020.
- [18] J. Liu, M. Yang, X. Xie, C. Peng, and H. Yan, "Finite-time H<sub>∞</sub> filtering for state-dependent uncertain systems with event-triggered mechanism and multiple attacks," *IEEE Trans. Circuits Syst. I, Reg. Papers*, vol. 67, no. 3, pp. 1021–1034, Nov. 2019, doi: [10.1109/TCSI.2019.2949014](https://doi.org/10.1109/TCSI.2019.2949014).
- [19] Q.-K. Li, X. Li, J. Wang, and S. Du, "Stabilization of networked control systems using a mixed-mode based switched delay system method," *IEEE/CAA J. Automatica Sinica*, vol. 5, no. 6, pp. 1089–1098, Nov. 2018.
- [20] H. Niu, A. Sahoo, C. Bhowmick, and S. Jagannathan, "An optimal hybrid learning approach for attack detection in linear networked control systems," *IEEE/CAA J. Automatica Sinica*, vol. 6, no. 6, pp. 1404–1416, Nov. 2019.
- [21] M. S. Mahmoud and M. M. Hamdan, "Fundamental issues in networked control systems," *IEEE/CAA J. Automatica Sinica*, vol. 5, no. 5, pp. 902–922, Sep. 2018.
- [22] B.-L. Zhang and Q.-L. Han, "Network-based modelling and active control for offshore steel jacket platform with TMD mechanisms," *J. Sound Vib.*, vol. 333, no. 25, pp. 6796–6814, Dec. 2014.
- [23] B.-L. Zhang, Q.-L. Han, and X.-M. Zhang, "Event-triggered H<sub>∞</sub> reliable control for offshore structures in network environments," *J. Sound Vib.*, vol. 368, pp. 1–21, Apr. 2016.
- [24] E. Fridman, "A refined input delay approach to sampled-data control," *Automatica*, vol. 46, no. 2, pp. 421–427, Feb. 2010.
- [25] W.-A. Zhang, H. Dong, G. Guo, and L. Yu, "Distributed sampled-data H<sub>∞</sub> filtering for sensor networks with nonuniform sampling periods," *IEEE Trans. Ind. Informat.*, vol. 10, no. 2, pp. 871–881, May 2014.
- [26] X.-M. Zhang and Q.-L. Han, "Event-triggered H<sub>∞</sub> control for a class of nonlinear networked control systems using novel integral inequalities," *Int. J. Robust Nonlinear Control*, vol. 27, no. 4, pp. 679–700, Mar. 2017.
- [27] P. Shi, H. Wang, and C.-C. Lim, "Network-based event-triggered control for singular systems with quantizations," *IEEE Trans. Ind. Electron.*, vol. 63, no. 2, pp. 1230–1238, Feb. 2016.
- [28] J. Wang, X.-M. Zhang, and Q.-L. Han, "Event-triggered generalized dissipativity filtering for neural networks with time-varying delays," *IEEE Trans. Neural Netw. Learn. Syst.*, vol. 27, no. 1, pp. 77–88, Jan. 2016.
- [29] L. Ding, Q.-L. Han, and X.-M. Zhang, "Distributed secondary control for active power sharing and frequency regulation in islanded microgrids using an event-triggered communication mechanism," *IEEE Trans. Ind. Informat.*, vol. 15, no. 7, pp. 3910–3922, Jul. 2019.
- [30] X. Ge, Q.-L. Han, D. Ding, X.-M. Zhang, and B. Ning, "A survey on recent advances in distributed sampled-data cooperative control of multi-agent systems," *Neurocomputing*, vol. 275, pp. 1684–1701, Jan. 2018.
- [31] X. Xie, Q. Zhou, D. Yue, and H. Li, "Relaxed control design of discrete-time Takagi–Sugeno fuzzy systems: An event-triggered real-time scheduling approach," *IEEE Trans. Syst., Man, Cybern. Syst.*, vol. 48, no. 12, pp. 2251–2262, Dec. 2018.
- [32] J. Liu, L. Zha, J. Cao, and S. Fei, "Hybrid-driven-based stabilisation for networked control systems," *IET Control Theory Appl.*, vol. 10, no. 17, pp. 2279–2285, Nov. 2016.
- [33] J. Liu, Z.-G. Wu, D. Yue, and J. H. Park, "Stabilization of networked control systems with hybrid-driven mechanism and probabilistic cyber attacks," *IEEE Trans. Syst., Man, Cybern. Syst.*, early access, Jan. 4, 2019, doi: [10.1109/TSMC.2018.2888633](https://doi.org/10.1109/TSMC.2018.2888633).
- [34] M. Sathishkumar and Y.-C. Liu, "Hybrid-triggered reliable dissipative control for singular networked cascade control systems with cyber-attacks," *J. Franklin Inst.*, Jan. 2020, doi: [10.1016/j.jfranklin.2020.01.013](https://doi.org/10.1016/j.jfranklin.2020.01.013).
- [35] J. Liu, Y. Gu, X. Xie, D. Yue, and J. H. Park, "Hybrid-driven-based H<sub>∞</sub> control for networked cascade control systems with actuator saturations and stochastic cyber attacks," *IEEE Trans. Syst., Man, Cybern. Syst.*, vol. 49, no. 12, pp. 2452–2463, Dec. 2019.
- [36] X.-M. Zhang and Q.-L. Han, "A decentralized event-triggered dissipative control scheme for systems with multiple sensors to sample the system outputs," *IEEE Trans. Cybern.*, vol. 46, no. 12, pp. 2745–2757, Dec. 2016.
- [37] C. Peng and M.-R. Fei, "An improved result on the stability of uncertain T–S fuzzy systems with interval time-varying delay," *Fuzzy Sets Syst.*, vol. 212, pp. 97–109, Feb. 2013.
- [38] L. Zhou, J. She, S. Zhou, and C. Li, "Compensation for state-dependent nonlinearity in a modified repetitive control system," *Int. J. Robust Nonlinear Control*, vol. 28, no. 1, pp. 213–226, Jan. 2018.
- [39] L. Zhou, J. She, X.-M. Zhang, Z. Cao, and Z. Zhang, "Performance enhancement of RCS and application to tracking control of chuck-workpiece systems," *IEEE Trans. Ind. Electron.*, vol. 67, no. 5, pp. 4056–4065, May 2020.



**EN-ZHI CAO** is currently pursuing the master's degree with China Jiliang University, Hangzhou, China. His current research interests include networked control systems and time-delay systems.





**ZHIHUI CAI** received the Ph.D. degree in mathematics from Zhejiang University, Hangzhou, China, in 2009. He is currently an Associate Professor with the Department of Applied Mathematics, China Jiliang University, Hangzhou. His current research interests include neural networks and time-delay systems.



**BINRUI WANG** received the Ph.D. degree in pattern recognition and intelligent system from Northeastern University, Shenyang, China, in 2005. He is currently a Professor and the Director of the Engineering Training Center, China Jiliang University, Hangzhou, China. His research interests include intelligent control algorithm and humanoid robot.

...



**BAO-LIN ZHANG** (Member, IEEE) received the Ph.D. degree in physical oceanography from the Ocean University of China, Qingdao, China, in 2006. He is currently a Professor and the Dean of the College of Science, China Jiliang University, Hangzhou, China. His current research interests include network-based control systems, time-delay systems, and vibration control systems.